

$^{12}\text{C}/^{13}\text{C}$ kinetic isotope effects of the gas-phase reactions of isoprene, methacrolein, and methyl vinyl ketone with OH radicals

Richard Iannone^{a,b}, Ralf Koppmann^{b,c}, Jochen Rudolph^{a,*}

A B S T R A C T

The stable-carbon kinetic isotope effects (KIEs) for the gas-phase reactions of isoprene, methacrolein (MACR), and methyl vinyl ketone (MVK) with OH radicals were studied in a 25 L reaction chamber at (298 ± 2) K and ambient pressure. The time dependence of both the stable-carbon isotope ratios and the concentrations was determined using a gas-chromatography combustion isotope ratio mass spectrometry (GCC-IRMS) system. The volatile organic compounds (VOCs) used in the KIE experiments had natural-abundance isotopic composition thus KIE data obtained from these experiments can be directly applied to atmospheric studies of isoprene chemistry. All $^{12}\text{C}/^{13}\text{C}$ KIE values are reported as ϵ values, where $\epsilon = (\text{KIE} - 1) \times 1000\text{‰}$, and $\text{KIE} = k_{12}/k_{13}$. The following average stable-carbon KIEs were obtained: $(6.56 \pm 0.12)\text{‰}$ (isoprene), $(6.47 \pm 0.27)\text{‰}$ (MACR), and $(7.58 \pm 0.47)\text{‰}$ (MVK). The measured KIEs all agree within uncertainty to an inverse molecular mass (MM) dependence of $\text{OH}\epsilon(\text{‰}) = (487 \pm 18)\text{MM}^{-1}$, which was derived from two previous studies [J. Geophys. Res. **2000**, *105*, 29329–29346; J. Phys. Chem. A **2004**, *108*, 11537–11544]. Upon adding the isoprene, MACR, and MVK $\text{OH}\epsilon$ values from this study, the inverse MM dependence changes only marginally to $\text{OH}\epsilon(\text{‰}) = (485 \pm 14)\text{MM}^{-1}$. The addition of these isoprene $\text{OH}\epsilon$ values to a recently measured set of $\text{O}_2\epsilon$ values in an analogous study [Atmos. Environ. **2008**, *42*, 8728–8737] allows for estimates of the average change in the $^{12}\text{C}/^{13}\text{C}$ ratio due to processing in the troposphere.

1. Introduction

It is now well known that the predominant emissions of biogenic volatile organic compound (VOC) hydrocarbons into the atmosphere are those of isoprene, where estimated annual emissions are $410\text{--}600 \text{ Tg yr}^{-1}$ (Guenther et al., 1995, 2006; Wang and Shallcross, 2000; Lathière et al., 2006; Müller et al., 2008). Isoprene emissions have significant effects on atmospheric chemistry such as their contribution toward ozone formation (Trainer et al., 1987; Fehsenfeld et al., 1992; Williams et al., 1997; Biesenhal et al., 1997) and aerosol formation (Claeys et al., 2004; Edney et al., 2005; Kroll et al., 2005; Henze and Seinfeld, 2006). Isoprene is synthesized by the action of isoprene synthase on dimethylallyl diphosphate (DMADP) produced by the methylerythritol 4-phosphate (MEP) pathway (Silver and Fall, 1991; Schwender et al., 1997). Isoprene emissions from leaves are light and temperature dependent (Sanadze, 1969, 2004; Tingey et al., 1979; Monson and Fall, 1989; Loreto and Sharkey, 1990), and use

carbon taken directly from the Calvin–Benson–Bassham cycle in leaf chloroplasts (Delwiche and Sharkey, 1993; Affek and Yakir, 2003; Schnitzler et al., 2004; Ferrieri et al., 2005).

In the atmosphere isoprene undergoes reactions with OH and NO_3 radicals, ozone, and halogen atoms; however, the reaction with OH greatly dominates. This is due to a combination of two factors: the temperature- and light-induced emissions of isoprene from vegetation temporally coincide with OH radical formation, and the reaction rate for the isoprene + OH is several magnitudes higher than that for both O_3 and NO_3 . Given the importance of the OH-initiated degradation pathway, a large number of studies dealing with kinetics (Paulson et al., 1992; Campuzano-Jost et al., 2000; Lee et al., 2005), reaction mechanisms (Miyoshi et al., 1994), and products (Tuazon and Atkinson, 1990; Kwok et al., 1995; Benkelberg et al., 2000; Ruppert and Becker, 2000; Sprengnether et al., 2002) have been published over the past two decades. Methacrolein (MACR), methyl vinyl ketone (MVK), 3-methylfuran, and formaldehyde are major products of the isoprene + OH reaction. Upon the formation, MACR and MVK are removed from the atmosphere through OH and O_3 oxidations, albeit at lower rates than for isoprene. Again, reaction with OH is by far the dominant removal

process for these isoprene products. Several studies have focused on ambient measurements of isoprene and its degradation products (Warneke et al., 2001; Stroud et al., 2001, 2002; Apel et al., 2002), however, given the complex dependence between isoprene, MACR, and MVK mixing ratios, it is difficult to estimate the sources or sinks of these volatile organic compounds (VOCs) through the use of atmospheric mixing ratio data alone.

Several recent studies have focused on the stable-carbon isotope ratios of atmospheric VOCs in order to obtain additional constraints on the processes that determine atmospheric VOC mixing ratios (Rudolph et al., 1997, 2003; Tsunogai et al., 1999; Saito et al., 2002; Goldstein and Shaw, 2003; Nara et al., 2006, 2007; Iannone et al., 2007). The application of $^{12}\text{C}/^{13}\text{C}$ studies toward determining the photochemical history of the studied VOC requires knowledge of the isotopic fractionations associated with its chemical removal processes (Rudolph and Czuba, 2000). Several experimental studies have contributed toward the development of a database of $^{12}\text{C}/^{13}\text{C}$ kinetic isotope effect (KIE) values associated with key gas-phase reactions (Rudolph et al., 2000; Iannone et al., 2003, 2008; Anderson et al., 2004a,b, 2007a,b). All of the previous studies employed gas-chromatography combustion isotope ratio mass spectrometry (GC-IRMS) instrumentation to analyze gas-phase reaction mixtures from Teflon chambers. A detailed description of the KIE measurement technique can be found in Anderson et al. (2003).

In this paper, we present and discuss measurements of the stable carbon KIEs for the gas-phase reactions of isoprene, MACR, and MVK with OH radicals. These KIE measurements complement the very recent analogous KIE study for these VOCs in reaction with ozone (Iannone et al., 2008). In both studies, measurements were made using VOCs without artificial enrichment or depletion of ^{13}C and thus their results are directly applicable to atmospheric reactions. The combination of KIE values for OH- and O_3 -initiated oxidations of these VOCs will allow for quantitative evaluation of their photochemical histories from the combination of isotope ratio and concentration measurements.

2. Experimental

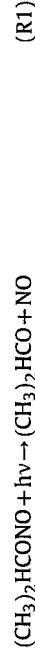
The gas chromatography combustion isotope ratio mass spectrometry (GCC-IRMS) technique used in this investigation is very similar to those described previously for the measurements of stable-carbon isotope KIE values (Anderson et al., 2004a,b, 2007a,b; Iannone et al., 2003, 2008). KIE experiments are similar in concept to relative rate (RR) experiments. In RR experiments, several reactants undergo chemical loss and their concentrations are measured as a function of time. However, in addition to concentration measurements, stable isotope ratios are also required for the calculation of KIE values. Thus, KIE values and RR can be determined in the same experiment. Two types of experiments were performed in this study: (1) RR experiments measuring only concentration values, and (2) KIE experiments measuring both concentrations and $^{12}\text{C}/^{13}\text{C}$ carbon isotope ratios. For the RR experiments, a GC-FID instrument was used; the KIE studies used a GCC-IRMS system. Fig. 1 provides a schematic for both systems, where the reaction chamber and the sample transfer system were common to both.

Reaction chambers were made from 0.05 mm thick FEP Teflon film. Several PTFE Teflon ports containing 9.5 mm diameter GC septa were used for introducing gases, extracting samples through a vacuum line, and injecting liquid-phase VOCs with a microliter syringe. A rotary fan, used to ensure VOC mixing, was suspended inside the chamber and its electrical leads were passed through two Teflon ports. The reaction chamber was suspended inside a temperature-controlled housing maintained at (298 ± 2) K. The

~ 0.1 m³ enclosure generally kept the reaction chamber in the dark but also allows for irradiation with up to twelve individually-controlled linear fluorescent, blacklight lamps with $\lambda_{\text{max}} = 350$ nm (F40T12/350BL, Osram Sylvania Inc., Danvers, Maine). Reaction chambers were replaced after every two experiments to avoid interference due to contaminating species that can accumulate on the chamber walls.

Two sets of reactions were carried out in separate RR and KIE experiments: (1) reactions of OH radicals with isoprene, and (2) the reaction of OH with MACR and MVK. For all experiments, *n*-heptane, *n*-octane, and *n*-nonane were used as reference compounds, for a few experiments also *p*-xylene was used as reference compound. Initial VOC mixing ratios were in the range of 10–18 ppmV. All liquid VOCs were obtained from Sigma–Aldrich with the following stated purities: isoprene (99%), MACR (95%), MVK (99%), *n*-heptane (99%), *n*-octane (98%), and *n*-nonane (99%), and *p*-xylene (99+%).

VOCs were injected into the chamber already containing 25 L of synthetic air (99.999% Praxair). Isopropyl nitrite (IPN) and NO were added to allow the photochemical production of OH radicals. IPN was synthesized in the laboratory using a procedure based on the syntheses of alkyl nitrites described by Noyes (1943) and Levin and Hartung (1995). Before initiating any OH-radical reactions by turning on the fluorescent lights in the chamber housing, 3–4 measurements were conducted in order to determine the stability of the VOC mixing ratios and the stable-carbon isotope ratios. Consecutive measurements of reaction chamber mixtures took 1–1.5 h, depending on amount of time for the separation and preparation of GC-IRMS instrument components for the subsequent measurement. Activating the UV lamps resulted in generation of OH radicals:



Depending upon the desired rate of reactant depletion, 5–60 μL of IPN were injected and 1–5 UV lamps were activated per run. Samples of reaction chamber air were taken through a 1/8" Teflon line at a flow rate of 35 mL min⁻¹ using a diaphragm pump. The sample flow proceeded through a six-port sampling valve and a 10 cm³ sampling loop. After the conditioning of the sample loop with 70 mL of chamber air, the position of six-port valve was pneumatically changed, transferring the 10 cm³ sample in He carrier gas to either the GC-FID (RR experiments) or GC-IRMS (KIE experiments).

The GC-FID measurements used a SiCHROMAT gas chromatograph (Siemens AG, Munich, Germany) equipped with a 15 m \times 5.0 μm film \times 0.53 mm i.d. RTX-5 column (Restek Corp., Bellefonte, PA). The initial GC temperature was isothermal at 303 K (held for 5.00 min), and increased at a rate of 5.00 K min⁻¹ until the final temperature of 393 K was reached and held for 7.00 min. A split ratio of 1:20 was used for the helium carrier gas (99.9999%, Messer) prior to entering the GC column. The column flow rate was 7 mL min⁻¹. VOC peak evaluations were performed using a PE Nelson 900 Series Interface (PerkinElmer Life and Analytical Sciences, Inc., Boston, MA) interfaced to a PC with a PE Nelson software package. Each VOC peak was integrated by manually defining the peak boundaries. For RR experiments, chamber samples were taken at regular intervals of 0.5 h and continued until the reactant VOCs were depleted to <25% of their initial concentrations, which typically occurred between 5 and 7 h. A mixture of MACR and MVK (in the Teflon chamber filled with 25 L of synthetic air) was monitored for concentration losses, with and without UV

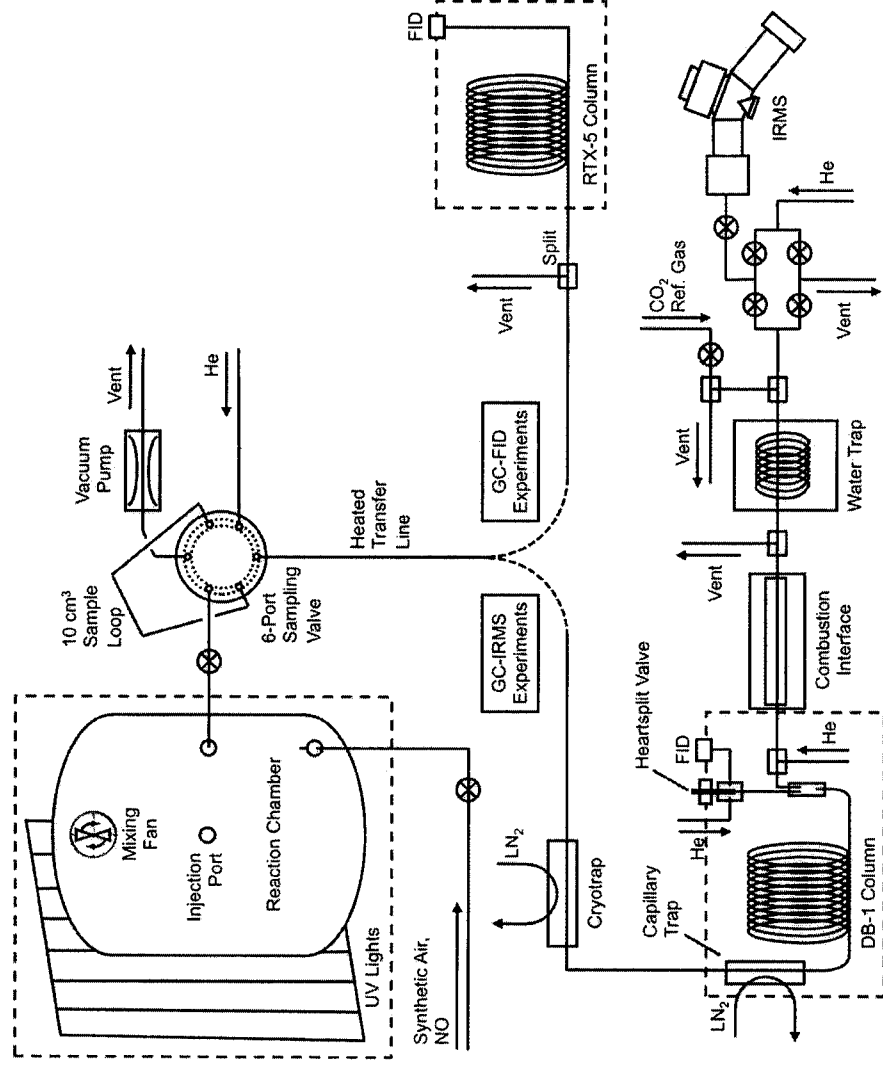


Fig. 1. System schematics used for relative rate (RR) and carbon kinetic isotope effect (KIE) experiments using GC-FID and GC-IRMS systems, respectively. For all GC-IRMS experiments, the heartsplit valve remained closed and all eluate from the DB-1 column was sent to the combustion furnace.

irradiation, in the absence of any IPN for about 45 h and 50 h, respectively.

The GC-IRMS measurements used the following combination of instruments: (1) a custom-built Online TDS G Large cryofocusing system (Gerstel GmbH & Co. KG, Mülheim an der Ruhr, Germany), (2) an Agilent 6890 Gas Chromatograph equipped with a 60 m \times 5 μ m film \times 0.32 mm i.d. DB-1 column (Agilent Technologies), (3) a combustion interface, (4) a water trap, and (5) an Isoprime Isotope Ratio Mass Spectrometer (IRMS) (GV Instruments, Manchester, UK). The cryotrap concentrated the VOCs at 163 K prior to injection onto the GC column by rapid heating. After injection, a column trap was used to focus the VOCs at the top of the capillary column at 213 K. The gas chromatograph used the following temperature program: 303 K held for 7.50 min, increased at a rate of 4.00 K min^{-1} until the final temperature of 373 K was reached, and held for 35 min (60 min total). The helium flow rate through the column was set to 1.8 mL min^{-1} for all runs. The VOCs eluting from the column were converted to CO_2 and water in the combustion interface, which consisted of a quartz tube packed with 0.1–0.5 mm Cu particles at an operating temperature of 1123 K. Water removal was performed by a water trap which consisting of a coiled capillary cooled with liquid nitrogen to 173 K.

The helium gas stream containing $^{12}\text{CO}_2$ and $^{13}\text{CO}_2$ enters the source of the IRMS through an open split at 0.4 mL min^{-1} . CO_2 was ionized and separated into three ion beams of m/z 44, 45, and 46, which were simultaneously detected in Faraday cup collectors. The resulting, amplified ion currents were continuously monitored and stored in digitized form for the evaluation of the isotope traces. For

every mass trace, peak areas were determined using IRMS integration software. CO_2 reference gas with $\delta^{13}\text{C}_{\text{V-PDB}} = -4.62\text{‰}$ was injected in pulses of 30 s duration near the beginning and end of every experiment (2 min and 58 min). Peaks representing separated VOCs in IRMS mass traces were automatically integrated using MassLynx v4.0i (GV Instruments). Reactant concentrations were proportional to the integrated peak areas of the m/z -44 trace and these peak area values were used to evaluate relative rate constants.

Relative rate constants were determined for all VOCs in the KIE and RR experiments. The relative rate is the ratio of rate constants, k_z/k_{ref} , for the studied VOC (VOC_z) and a reference VOC (VOC_{ref}). It was determined through the following equation:

$$\ln\left(\frac{[\text{VOC}_z]_0}{[\text{VOC}_z]_t}\right) = \frac{k_z}{k_{\text{ref}}} \ln\left(\frac{[\text{VOC}_{\text{ref}}]_0}{[\text{VOC}_{\text{ref}}]_t}\right) \quad (1)$$

where $[\text{VOC}_z]_0$ and $[\text{VOC}_{\text{ref}}]_0$ were taken as average concentrations of the VOCs determined before any reactions were initiated, and $[\text{VOC}_z]_t$ and $[\text{VOC}_{\text{ref}}]_t$ were concentration measurements during VOC loss. The relative rate was determined through a linear regression analysis of $\ln([\text{VOC}_z]_0/[\text{VOC}_z]_t)$ against $\ln([\text{VOC}_{\text{ref}}]_0/[\text{VOC}_{\text{ref}}]_t)$, where the slope was k_z/k_{ref} . The experimental rate constant, k_{RR} , was determined through multiplication of the slope k_z/k_{ref} with the literature rate constant of the reference compound, k_{ref} . The experimental uncertainty of k_{RR} was determined from the standard error of the slope of Equation (1) and the reported uncertainty of k_{ref} .

Stable-carbon delta values and VOC peak areas were used to determine $^{12}\text{C}/^{13}\text{C}$ KIEs from GCC-IRMS measurements. The stable-carbon isotope form of the KIE is equivalent to the ratio k_{12}/k_{13} where, given the same reaction, k_{12} is the rate constant for the reactant containing solely ^{12}C atoms and k_{13} is the rate constant for the same reactant substituted with one ^{13}C atom. The KIE was determined from the slope of a linear dependence between the concentration and stable-carbon isotope ratio of the studied VOC (Rudolph et al., 2000; Anderson et al., 2003) using the following equation:

$$\ln \left(\frac{[^{12}\text{C}]_{s,t}}{[^{12}\text{C}]_{s,0}} \right) = \frac{k_{12}/k_{13}}{1 - k_{12}/k_{13}} \ln \left(\frac{\delta^{13}\text{C}_t + 1000\text{‰}}{\delta^{13}\text{C}_0 + 1000\text{‰}} \right) \quad (2)$$

Here, the integrated VOC peak areas from the m/z -44 signal trace are proportional to the concentration values for the sample compound $[^{12}\text{C}]_{s,t}$ and $[^{12}\text{C}]_{s,0}$. The quantities $\delta^{13}\text{C}_t$ and $\delta^{13}\text{C}_0$ are stable-carbon isotope ratio delta values expressed as per mille difference values relative to V-PDB (Vienna Pee Dee Belemnite). Equation (2) was plotted as $\ln([^{12}\text{C}_t/^{12}\text{C}_0])$ against $\ln[(\delta^{13}\text{C}_t + 1000\text{‰})/(\delta^{13}\text{C}_0 + 1000\text{‰})]$ where a straight line was formed with a zero y -axis intercept. Given the definition of the carbon KIE as k_{12}/k_{13} , the slope $(k_{12}/k_{13})/(1 - k_{12}/k_{13})$ of Equation (2) allowed for the determination of the KIE using.

$$\text{KIE} = \frac{\text{slope}}{1 + \text{slope}} \quad (3)$$

A final calculation transforms the KIE into the commonly used epsilon value:

$$\epsilon = - \left(\frac{k_{12}}{k_{13}} - 1 \right) 1000\text{‰} \quad (4)$$

3. Results and discussion

3.1. Wall losses, relative rate experiments, and determination of KIEs

First-order loss rate constants of $(1.25 \pm 0.07) \times 10^{-6} \text{ s}^{-1}$ and $(7.86 \pm 0.07) \times 10^{-7} \text{ s}^{-1}$ were determined for MACR and MVK, respectively, in the absence of lighting inside the 25 L chamber. Cross-sections for MACR and MVK (260–390 nm) partially overlap with the emission spectra of the UV lamps inside the reaction chamber enclosure, which have an emission maximum at 350 nm (Fig. 2). Since UV radiation of the reaction mixture was required for

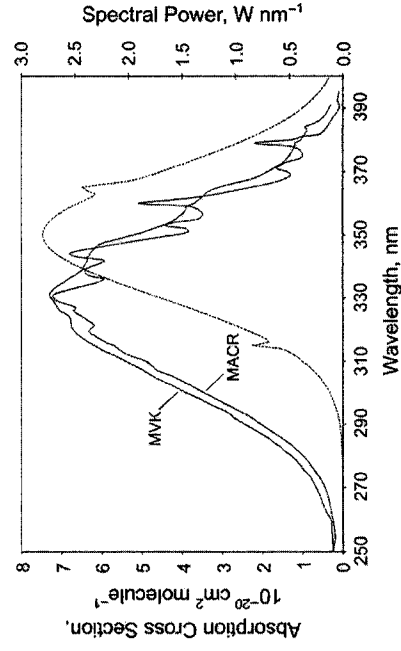


Fig. 2. Absorption cross-sections of MACR and MVK at 298 K. Also shown is the spectral power distribution for the F40/350BL fluorescent lamp. Cross-section data taken from Gierczak et al., (1997); lamp data provided by Osram Sylvania Inc.

the *in situ* generation of OH radicals in RR and KIE experiments according to Reaction (R1), studies of the photolytic loss of MACR and MVK in the absence of OH radicals were conducted. From the experiments irradiating mixtures of MVK and MACR in synthetic air in the absence of IPN, photolytic loss rates were determined. MACR experienced a loss rate that was within the uncertainty of the measurement identical to the wall loss rate. For MVK the results indicate a small photolytic loss leading to an overall first-order loss rate constant (wall loss + photolysis) of $1.0 \times 10^{-6} \text{ s}^{-1}$. For the typical duration of the RR and KIE experiment of 8–10 h, these losses would contribute ~4% and ~2.5% to the total loss of MACR and MVK, respectively. The measured peak areas of MACR and MVK were corrected for these losses.

Statistics were determined for repeat pre-reaction measurements of VOCs for all experiments performed. From 28 individual measurements of the VOC mixture inside the reaction chamber (from a total of 10 KIE experiments), the mean relative standard deviation for peak areas was 1.20% and the mean standard deviation for $\delta^{13}\text{C}$ values was 0.37‰. The corresponding 95% confidence intervals are (0.04–2.15%) and (0.05–0.63)‰ for standard deviations of peak areas and $\delta^{13}\text{C}$ values, respectively. These variations in integrated peak area and $\delta^{13}\text{C}$ are within expected error bounds for this type of instrumentation and have been observed in previous KIE studies (e.g. Iannone et al., 2003; Anderson et al., 2003, 2007a,b). These variations are small compared to the overall changes that occur from the reaction of the chamber VOCs with OH radicals.

Relative rate comparisons were conducted for selected VOCs within both the GC-FID and GC-IRMS experiments. Fig. 3 provides an example of a relative rate plot for the reactions of MACR, MVK, *n*-heptane, and *n*-octane with OH radicals using *n*-heptane as reference VOC. The uncertainty for each experimentally-determined k_{RR} value was derived from the standard error of the relative rate analysis, and the uncertainty of the reference compound. Uncertainties associated with mean values for k_{RR} were determined from 1σ standard errors. A summary of mean experimental rate constants (k_{RR}), and comparisons to literature values, is provided in Table 1. From GC-FID data, all k_{RR} values agree, within the uncertainty of the measurements, with literature rate constants except in the case of *n*-hexane. It should be noted that a relatively high uncertainty in k_{RR} for this reaction was determined in comparison, the average k_{RR} values obtained from GC-IRMS data are similar but have lower uncertainties due to

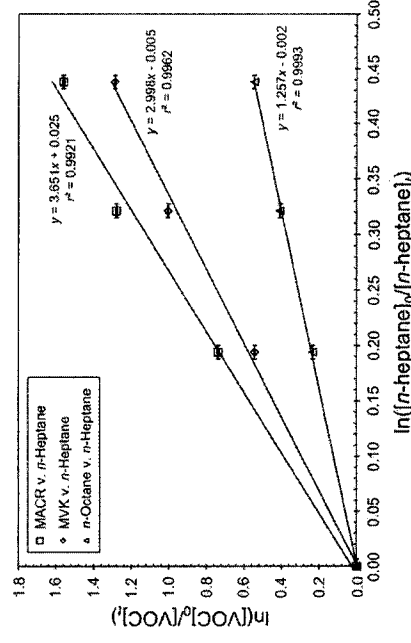


Fig. 3. Example of a relative rate plot for the reactions of MACR, MVK, and *n*-octane with OH radicals in a GCC-IRMS experiment, using *n*-heptane as the reference VOC. Slopes correspond to k_i/k_{ref} , which were used to determine the relative rate constants k_{RR} for each VOC + OH reaction.

Table 1

Comparison between mean relative rate constants from the GC-FID and GCC-IRMS studies of this investigation and literature rate constants (298 K).

Studied VOC	$k_{OH}, 10^{-11} \text{ cm}^3 \text{ molecule}^{-1} \text{ s}^{-1}$			Literature Value
	This work, GC-FID	This work, GCC-IRMS	This work, GCC-IRMS	
Isoprene	11.5 ± 3.50	12.6 ± 1.34	10.1 ± 2.5^a	
MACR	2.74 ± 0.71	3.43 ± 0.10	3.35 ± 0.84^b	
MVK	2.06 ± 0.55	3.09 ± 0.10	1.88 ± 0.47^b	
n-Hexane	0.90 ± 0.25	-	0.55 ± 0.08^a	
n-Heptane	0.68 ± 0.19	0.59 ± 0.05	0.70 ± 0.11^a	
n-Octane	0.79 ± 0.21	0.85 ± 0.08	0.87 ± 0.01^a	
n-Nonane	-	1.00 ± 0.03	1.00 ± 0.15^a	
p-Xylene	1.33 ± 0.48	1.02 ± 0.21	1.30 ± 0.20^c	

^a Atkinson (1997).

^b Aschmann and Atkinson (1994).

^c Atkinson and Aschmann (1989).

better agreement of repeat measurements. The k_{OH} value determined for the MVK + OH reaction, is slightly above the range of values expected from literature and GC-FID results. However wall losses and photolysis, being very small, cannot explain such a discrepancy. Nevertheless, the results confirm the expectation that the measured changes in VOC concentrations are indeed due to reaction with the OH radical.

Fig. 4 provides an example of a KIE determination through the least-squares analysis of several data points and the subsequent calculations required to obtain the OH_{ϵ} value. Linear-regression analyses used a simple regression model and thus did not consider the individual errors of the data points. Those data points resulting from integrations where peak overlaps were observed were excluded from the fit procedure. Nevertheless, four or more data points were available for every KIE evaluation and r^2 values were often above 0.99 and reactants typically underwent >60% depletion (>80% for isoprene). Table 2 provides a summary of OH_{ϵ} values determined in this study. Uncertainties of mean OH_{ϵ} values were based on standard errors of the mean (1σ). Errors for individual OH_{ϵ} values were determined using the standard error of the slope from the linear-regression analysis.

3.2. Comparison with previously published data

The average isoprene OH_{ϵ} value of $(6.56 \pm 0.12)\%$ from this study is similar to the only other reported values of $(8.23 \pm 0.97)\%$, $(6.18 \pm 0.22)\%$, and $(6.40 \pm 0.24)\%$ (Rudolph et al., 2000). The 95% confidence interval of 6.10–6.80% for the five measurements

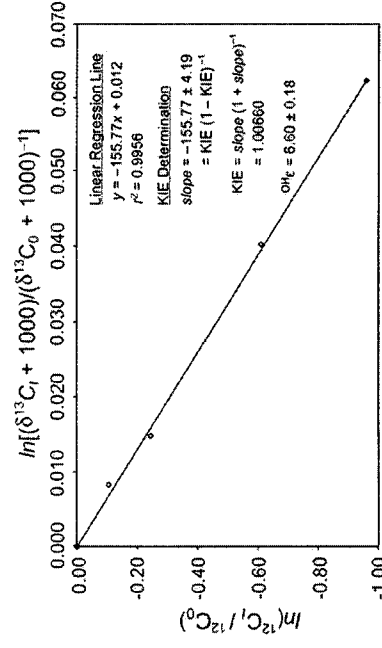


Fig. 4. Example of the graphical determination of stable-carbon KIE value for the isoprene + OH reaction through a least-squares analyses. The slope of Equation (2) is equivalent to the slope of the linear-regression line and was used to obtain the KIE value.

Table 2

Summary of stable carbon OH_{ϵ} values for the reactions of isoprene, MACR, and MVK with OH radicals at (298 ± 4) K.

Compound	Extent of Reaction, %	Number of Points	r^2 Statistic from KIE Plot	OH_{ϵ} , %
Isoprene	94.3	5	0.9993	6.46 ± 0.10
	85.6	4	0.9986	6.89 ± 0.18
	88.1	6	0.9959	6.24 ± 0.20
	77.1	4	0.9985	6.60 ± 0.18
	83.3	6	0.9997	6.60 ± 0.05
	Mean:			6.56 ± 0.12^a
95% Confidence Interval:				6.10–6.80
MACR	58.2	6	0.9853	7.14 ± 0.44
	80.5	6	0.9884	5.66 ± 0.31
	86.1	5	0.9985	6.37 ± 0.25
	55.9	5	0.9895	6.37 ± 0.39
	61.7	7	0.9998	6.74 ± 0.20
	Mean:			6.47 ± 0.27^a
95% Confidence Interval:				5.40–7.00
MVK	66.4	6	0.9990	8.83 ± 0.24
	83.6	6	0.9989	6.71 ± 0.12
	87.5	5	0.9975	6.89 ± 0.20
	56.2	5	0.9925	7.13 ± 0.65
	63.7	6	0.9983	8.33 ± 0.44
	Mean:			7.58 ± 0.47^a
95% Confidence Interval:				5.73–8.50

^a Uncertainty was determined by the standard error: $\sigma(n-1)^{-0.5}$, where σ represents the standard deviation of the averaged OH_{ϵ} values, and n represents the number of OH_{ϵ} values included in the calculation of the mean.

reported here agree with two measurements from the previous study. The uncertainty for the isoprene + OH KIE value of $(8.23 \pm 0.97)\%$ was due to the relatively poor fit of the data points to the linear dependence of equation (2), whereby the r^2 value was 0.9552 (the other two values exhibited r^2 values >0.995). Considering this and the new OH_{ϵ} values for isoprene presented here, the higher value of $(8.23 \pm 0.97)\%$ from the previous study probably is an experimental outlier. Excluding this outlier, an average value of $(6.56 \pm 0.12)\%$ was obtained.

In several previous KIE studies for specific gas-phase reactions (e.g. n-alkanes + OH, alkenes + O_3 , etc.), KIE values were fitted as a function of the inverse carbon number, N_C^{-1} (Rudolph et al., 2000; Iannone et al., 2003, 2008; Anderson et al., 2004a,b, 2007a,b). As can be seen from Fig. 5a the average isoprene OH_{ϵ} value from this study agrees within its uncertainty with predictions from the 1-alkene KIE dependence of $OH_{\epsilon}(\%) = (34.9 \pm 1.2)N_C^{-1}$, which can be derived from six KIE values reported by Rudolph et al. (2000) and one from Anderson et al. (2004b).

To date, there are no previously published KIE values for the reactions of MVK and MACR with OH radicals. The average OH_{ϵ} values for MACR and MVK are both lower than predicted from the N_C^{-1} KIE dependence. This is similar to the findings reported by Iannone et al. (2008) for the KIEs of the reaction of MVK and MACR with ozone. Iannone et al. (2008) showed that an inverse dependence on molecular mass (MM) will also provide a useful approximation. Specifically, the MM^{-1} KIE dependence provides a better prediction for the KIEs of the MACR and MVK reaction with ozone. Fig. 5b provides a comparison of available KIE data with a fit of the KIEs for reactions of 1-alkenes with OH radicals to a MM^{-1} dependence ($OH_{\epsilon}(\%) = (487 \pm 18) MM^{-1}$). Indeed, similar to the ozone reaction KIEs, the MM^{-1} dependence also provides a better prediction of the OH radical reaction KIEs for MVK and MACR.

A general comparison of the KIEs for reaction of alkenes with OH radicals and those for reaction with ozone reveals that the OH radical and ozone reaction KIEs are of similar magnitude (Fig. 6). The data points are very close to the 1:1 line and for very few data points the difference between measurements and a 1:1 correspondence

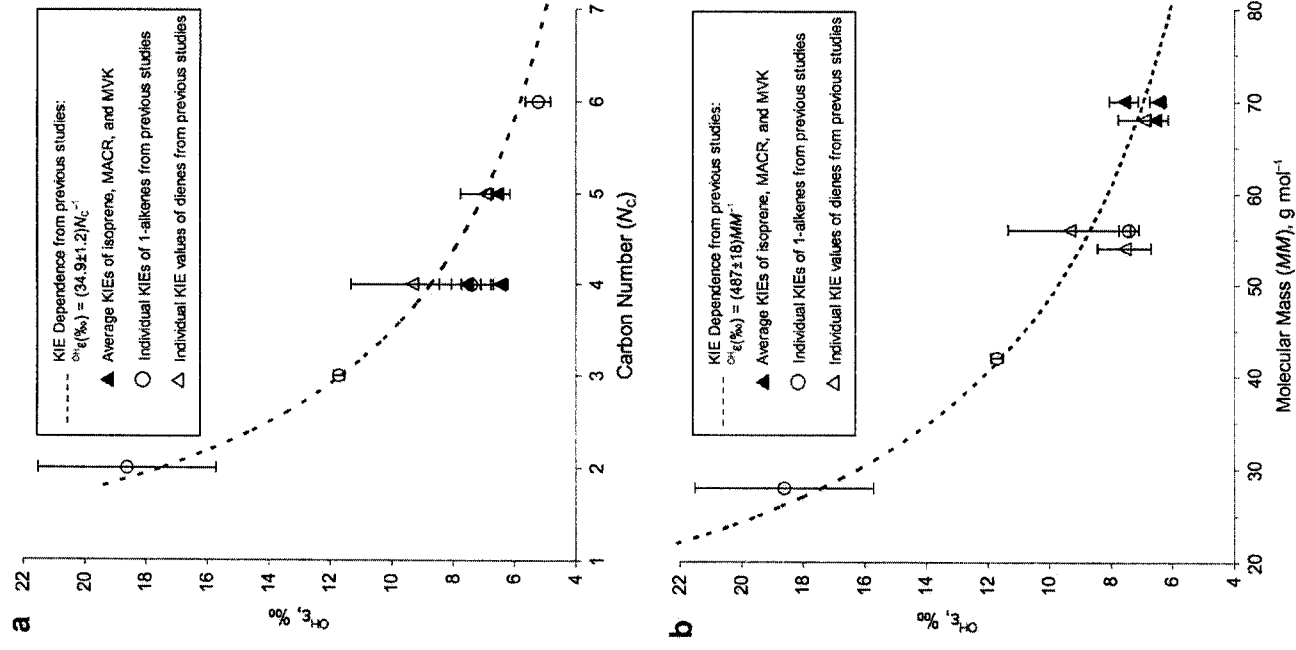


Fig. 5. Dependence of 1-alkene and diene OH_ϵ values to the inverse carbon number (NC^{-1} , graph a) and inverse molecular mass (MM^{-1} , graph b). The fit equations are $\text{OH}_\epsilon(\text{‰}) = (34.9 \pm 1.2) \text{NC}^{-1}$ and $\text{OH}_\epsilon(\text{‰}) = (487 \pm 18) \text{MM}^{-1}$ for graphs a and b, respectively. Previously published data provided by Rudolph et al. (2000) and Anderson et al. (2004b).

exceeds the experimental uncertainties. This may be partly due to the substantial uncertainties of the KIE values, which were taken from 2σ standard errors of mean values. Nevertheless, even for $\text{O}_3\text{-OH}_\epsilon$ data pairs with low uncertainties, the difference between OH radical and ozone reaction KIEs is small. For example the $\text{O}_3\text{-OH}$ values of $(8.38 \pm 0.42)\text{‰}$ for MACR, $(8.01 \pm 0.07)\text{‰}$ for MVK, and $(8.40 \pm 0.11)\text{‰}$ for isoprene reported by Iannone et al. (2008) are higher than the corresponding OH_ϵ values of $(6.47 \pm 0.27)\text{‰}$ (MACR), $(7.58 \pm 0.47)\text{‰}$ (MVK) and $(6.56 \pm 0.12)\text{‰}$ (isoprene) from this study. Based on the uncertainties, these differences cannot be

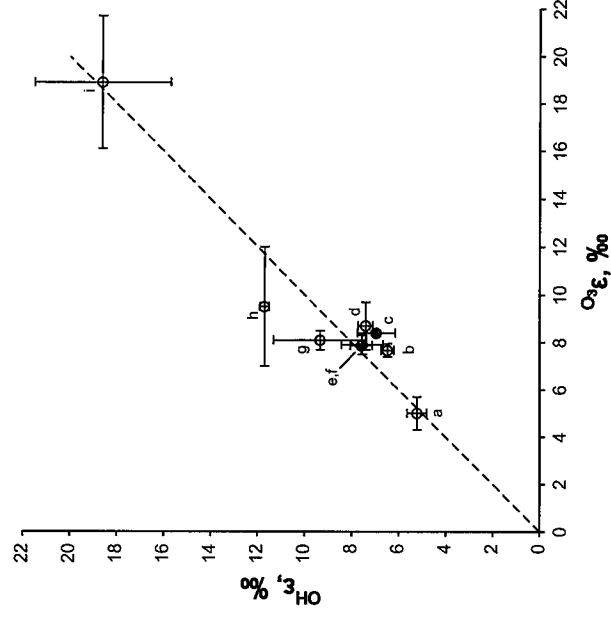


Fig. 6. Comparison between OH_ϵ and $\text{O}_3\text{-}\epsilon$ values for alkene-OH and alkene- O_3 reactions, respectively, from this and previous studies (see text for references). The alkenes are: (a) 1-hexene, (b) MACR, (c) isoprene, (d) 1-butene, (e) 1,3-butadiene, (f) MVK, (g) E-2-butene, (h) propene, and (i) ethene. The dashed line represents a hypothetical perfect agreement between the OH_ϵ and $\text{O}_3\text{-}\epsilon$ values.

completely explained by experimental errors. However, these differences are still less than 2%.

It is beyond the scope of this paper to discuss the implication that this finding has for the interpretation of details of the chemical mechanisms causing isotope fractionation during reaction of alkenes with ozone and OH radicals. However, as will be seen in the following section these similarities in magnitude for OH_ϵ and $\text{O}_3\text{-}\epsilon$ will have an important impact on the interpretation of isotope ratio measurements for MVK, MACR, isoprene and other alkenes in the troposphere.

3.3. Application of KIEs toward interpretations of ambient studies of VOCs

The change in the isotopic composition of an alkene relative to its source composition can be calculated by:

$$\delta^{13}\text{C} = \text{OH}_k \times \text{OH}_\epsilon(t \times [\text{OH}])_{\text{av}} + \text{O}_3k \times \text{O}_3\text{-}\epsilon(t \times [\text{O}_3])_{\text{av}} + \delta^{13}\text{C} \quad (5)$$

where $-\delta^{13}\text{C}$ and $\delta^{13}\text{C}$ represent observed and emitted carbon delta values for the alkene, respectively; $(t[\text{OH}])_{\text{av}}$ and $(t[\text{O}_3])_{\text{av}}$ represent the products of the average age of the alkene and the average concentrations of OH radicals and ozone, respectively; OH_k and $\text{O}_3\text{-}\epsilon$ are rate constants for reactions of OH and O_3 with the alkene, respectively; and OH_ϵ and $\text{O}_3\text{-}\epsilon$ are KIE values for reactions of OH and O_3 with the alkene, respectively.

The KIE comparison in Fig. 6 indicates that for alkenes the relative difference between OH_ϵ and $\text{O}_3\text{-}\epsilon$ generally is less than 25%. Consequently the change in isotope ratio due to photochemical processing ($\delta^{13}\text{C}-\delta^{13}\text{C}$) will depend only to a minor extent on the type of reaction. Even in extreme cases of the loss being entirely due to either ozone or OH radical reaction the change in isotope ratio will vary by 2.5% or less. The accuracy of presently available methods for isotope ratio measurements of VOCs is typically in the range of 0.5–2% ‰ , depending on available sample volume, compound, and

atmospheric mixing ratio. When considering the additional uncertainty created by possible variations in isotope signatures of VOC sources, it is evident that reliably determining the change in isotope ratios between emission and observation with a relative accuracy substantially better than 25% will only be possible in exceptional cases.

While the similar magnitude of the O₃- and OH-reaction KIEs seriously limits the use of isotope ratio measurements to identify the type of alkene loss reactions, it significantly improves the possibility of using isotope ratio measurements to differentiate between chemical loss and mixing processes as cause for changes in VOC mixing ratios. Using $\delta^{13}\text{C} \approx \delta^{13}\text{C}_0 \approx \epsilon$ we can modify Equation (5):

$$\delta^{13}\text{C} = \epsilon \left[\frac{[\text{OH}]_{\text{av}}}{[\text{OH}]} + \frac{[\text{O}_3]_{\text{av}}}{[\text{O}_3]} k(t \times [\text{O}_3])_{\text{av}} \right] + \delta^{13}\text{C}_0 \quad (6)$$

Since $\delta^{13}\text{C}(t[\text{OH}])_{\text{av}} + \text{O}_3 k(t[\text{O}_3])_{\text{av}}$ describes the combined loss due to reaction of the alkene with O₃ and OH radicals, Equation (6) can be explained by chemical processing alone, that is in the absence of mixing and dilution processes.

4. Conclusions

The KIE for reaction of isoprene with OH radicals determined in this study is consistent with previously reported measurements by Rudolph et al. (2000). The higher reproducibility of these new measurements allows for the determination of a substantially improved best estimate of $\epsilon = (6.56 \pm 0.12)\%$ for this reaction. The MACR and MVK $\delta^{13}\text{C}$ values are the first measurements of this kind reported in literature. Combined with the recently published KIEs for the corresponding ozone reactions, this provides the necessary information to use isotope ratio measurements to study some of the processes determining the atmospheric mixing ratios of isoprene as well as MVK and MACR. Specifically, isotope ratio measurements will be useful to quantitatively differentiate between the influence of chemical loss and mixing on changes in the atmospheric mixing ratios of isoprene, MVK, and MACR, as well as of other alkenes.

The semi-empirical relations between carbon number or molecular mass and KIE allow predictions of ϵ values with the necessary accuracy to be used in quantitative evaluations of the photochemical age of alkenes. Moreover, the KIEs for reaction of light alkenes, isoprene, MVK and MACR with OH radicals are large enough to result in measurable changes in carbon isotope ratios as consequence of atmospheric processing.

The finding that carbon KIEs for reactions of alkenes with OH radicals are very similar in magnitude to the KIEs for the corresponding reactions with ozone has important consequences. Carbon isotope ratio measurements will not be well suited for differentiating between alkene loss due to reaction with ozone or OH radicals. However, since reaction with ozone or the OH radicals are the only relevant atmospheric loss reactions for most alkenes, isotope ratio data can be very valuable to obtain insight into the role of loss processes in determining the atmospheric mixing ratios of alkenes. Specifically, it is expected that combining isotope ratio and mixing ratio measurements will help to quantify the contribution of photochemical loss processes to observed changes in mixing ratios.

References

- Affek, H.P., Yalir, D., 2003. Natural abundance carbon isotope composition of isoprene reflects incomplete coupling between isoprene synthesis and photo-synthetic carbon flow. *Plant Physiol.* 131, 1–10.
- Anderson, R.S., Czuba, E., Ernst, D., Huang, L., Thompson, A.E., Rudolph, J., 2003. Method for measuring carbon kinetic isotope effects of gas-phase reactions of light hydrocarbons with the hydroxyl radical. *J. Phys. Chem. A* 107, 6191–6199.
- Anderson, R.S., Iannone, R., Thompson, A.E., Rudolph, J., Huang, L., 2004a. Carbon kinetic isotope effects in the gas-phase reactions of aromatic hydrocarbons with the OH radical at 296 ± 4 K. *Geophys. Res. Lett.* 31, L15108. doi:10.1029/2004GL020089.
- Anderson, R.S., Huang, L., Iannone, R., Thompson, A.E., Rudolph, J., 2004b. Carbon kinetic isotope effects in the gas phase reactions of light alkenes and ethene with the OH radical at 296 ± 4 K. *J. Phys. Chem. A* 108, 11537–11544.
- Anderson, R.S., Huang, L., Iannone, R., Rudolph, J., 2007a. Measurements of the $^{12}\text{C}/^{13}\text{C}$ kinetic isotope effects in the gas-phase reactions of light alkenes with chlorine atoms. *J. Phys. Chem. A* 111, 495–504.
- Anderson, R.S., Huang, L., Iannone, R., Rudolph, J., 2007b. Laboratory measurements of the $^{12}\text{C}/^{13}\text{C}$ kinetic isotope effects in the gas-phase reactions of unsaturated hydrocarbons with Cl atoms at 298 ± 3 K. *J. Atmos. Chem.* 56, 275–291.
- Apel, E.C., Riemer, D.D., Hills, A., Baugh, W., Orlando, J., Faloon, I., Tan, D., Brune, W., Lamb, B., Westberg, H., Carroll, M.A., Thornberry, T., Geron, C.D., 2002. Measurement and interpretation of isoprene fluxes and isoprene, methacrolein, and methyl vinyl ketone mixing ratios at the PROPHET site during the 1998 Intensive. *J. Geophys. Res.* 107, 4034. doi:10.1029/2000JD000225.
- Aschmann, S.M., Atkinson, R., 1994. Formation yields of methyl vinyl ketone and methacrolein from the gas-phase reaction of O₃ with isoprene. *Environ. Sci. Technol.* 28, 1539–1542.
- Atkinson, R., 1997. Gas-phase tropospheric chemistry of volatile organic compounds. 1. Alkenes and alkenes. *J. Phys. Chem. Ref. Data* 26, 215–290.
- Atkinson, R., Aschmann, S.M., 1989. Rate constants for the gas-phase reactions of the OH radical with a series of aromatic hydrocarbons at 296 ± 2 K. *Int. J. Chem. Kinet.* 21, 355–365.
- Benkeberg, H., Böge, O., Seuwen, R., Warneke, P., 2000. Product distributions from the OH radical-induced oxidation of but-1-ene, methyl-substituted but-1-enes and isoprene in NO₂-free air. *Phys. Chem. Chem. Phys.* 2, 4029–4039.
- Biesenthal, T.A., Wu, Q., Shepson, P.B., Wiebe, H.A., Anlauf, K.G., Mackay, G.I., 1997. A study of relationships between isoprene, its oxidation products, and ozone, in the Lower Fraser Valley, BC. *Atmos. Environ.* 31, 2049–2058.
- Campuzano-Jost, P., Williams, M.B., D'Oro, L., Hynes, A.J., 2000. Kinetics of the OH-initiated oxidation of isoprene. *Geophys. Res. Lett.* 27, 693–696.
- Claeys, M., Graham, B., Vas, G., Wang, W., Vermeylen, R., Pashynska, V., Cafmeyer, J., Guyon, P., Andreae, M.O., Artaxo, P., Maenhaut, W., 2004. Formation of secondary organic aerosols through photooxidation of isoprene. *Science* 303, 1173–1176.
- Delwiche, C.F., Sharkey, T.D., 1993. Rapid appearance of ^{13}C in biogenic isoprene when $^{13}\text{CO}_2$ is fed to intact leaves. *Plant Cell Environ.* 16, 587–591.
- Edney, E., Kleindienst, T., Jaoui, M., Lewandowski, M., Offenberg, J.H., Wang, W., Claeys, M., 2005. Formation of 2-methyl tetrols and 2-methylglyceric acid in secondary organic aerosol from laboratory irradiated isoprene/NO₂/SO₂/air mixtures and their detection in ambient PM_{2.5} samples collected in the eastern United States. *Atmos. Environ.* 39, 5281–5289.
- Fehsenfeld, F.C., Calvert, J., Fall, R., Goldan, P., Guenther, A.B., Hewitt, C.N., Lamb, B., Liu, S., Trainer, M., Westberg, H., Zimmerman, P., 1992. Emissions of volatile organic compounds from vegetation and the implications for atmospheric chemistry. *Global Biogeochem. Cycles* 6, 389–430.
- Ferrier, R.A., Gray, D.W., Babst, B.A., Schueller, M.J., Schlyer, D.J., Thorpe, M.R., Orians, C.M., Lerdau, M., 2005. Use of carbon-11 in *Populus* shows that exogenous jasmonic acid increases biosynthesis of isoprene from recently fixed carbon. *Plant Cell Environ.* 28, 591–602.
- Gierczak, T., Burkholder, J.B., Talukdar, R.K., Mellouki, A., Barone, S.B., Ravishankara, A.R., 1997. Atmospheric fate of methyl vinyl ketone and methacrolein. *J. Photochem. Photobiol. A: Chem.* 110, 1–10.
- Goldstein, A.H., Shaw, S.L., 2003. Isotopes of volatile organic compounds: an emerging approach for studying atmospheric budgets and chemistry. *Chem. Rev.* 103, 5025–5048.
- Guenther, A., Hewitt, C.N., Erickson, D., Fall, R., Geron, C., Graedel, T., Harley, P., Klinger, L., Lerdau, M., McKay, W.A., Pierce, T., Scholes, B., Steinbrecher, R., Tallamraju, R., Taylor, J., Zimmerman, P., 1995. A global model of natural volatile organic compound emissions. *J. Geophys. Res.* 100, 8873–8892.
- Guenther, A., Karl, T., Harley, P., Wiedinmyer, C., Palmer, P.I., Geron, C., 2006. Estimates of global terrestrial isoprene emissions using MEGAN (Model of Emissions of Gases and Aerosols from Nature). *Atmos. Chem. Phys.* 6, 3181–3210.
- Henze, D.K., Seinfeld, J.H., 2006. Global secondary organic aerosol from isoprene oxidation. *Geophys. Res. Lett.* 33, L09812. doi:10.1029/2006GL025976.
- Iannone, R., Anderson, R.S., Rudolph, J., Huang, L., Ernst, D., 2003. The carbon kinetic isotope effects of ozone-alkene reactions in the gas-phase and the impact of ozone reactions on the stable carbon isotope ratios of alkenes in the atmosphere. *Geophys. Res. Lett.* 30, 1684. doi:10.1029/2003GL017221.
- Iannone, R., Koppmann, R., Rudolph, J., 2007. A technique for atmospheric measurements of stable carbon isotope ratios of isoprene, methacrolein, and methyl vinyl ketone. *J. Atmos. Chem.* 58, 181–202.

- Iannone, R., Koppmann, R., Rudolph, J., 2008. The stable carbon kinetic isotope effects of the reactions of isoprene, methacrolein, and methyl vinyl ketone with ozone in the gas phase. *Atmos. Environ.* 42, 8728–8737.
- Kroll, J., Ng, N., Murphy, S., Flagan, R., Seinfeld, J., 2005. Secondary organic aerosol formation from isoprene photooxidation under high-NO_x conditions. *Geophys. Res. Lett.* 32, L18808. doi:10.1029/2005GL023637.
- Kwok, E.S.C., Atkinson, R., Arey, J., 1995. Observation of hydroxycarbonyls from the OH radical-initiated reaction of isoprene. *Environ. Sci. Technol.* 29, 2467–2469.
- Lathière, J., Hauglustaine, D., Friend, A., De Noblet-Ducoudré, N., Viovy, N., Polberth, G.A., 2006. Impact of climate variability and land use changes on global biogenic volatile organic compound emissions. *Atmos. Chem. Phys.* 6, 2129–2146.
- Lee, L., Baasandorj, M., Stevens, P.S., Hites, R.A., 2005. Monitoring OH-initiated oxidation kinetics of isoprene and its products using online mass spectrometry. *Environ. Sci. Technol.* 39, 1030–1036.
- Levin, N., Hartung, W., 1995. *Organic Syntheses Collective*. Wiley, New York, pp. 92–103.
- Loreto, F., Sharkey, T., 1990. A gas-exchange study of photosynthesis and isoprene emission in *Quercus rubra* L. *Planta* 182, 523–531.
- Miyoshi, A., Hatakeyama, S., Washida, N., 1994. OH radical-initiated photooxidation of isoprene: an estimate of global CO production. *J. Geophys. Res.* 99, 18779–18787.
- Monson, R., Fall, R., 1989. Isoprene emission from aspen leaves: influence of environment and relation to photosynthesis and photorespiration. *Plant Physiol.* 90, 267–274.
- Müller, J.-F., Stavrakou, T., Wallens, S., De Smedt, I., Van Roozendael, M., Potosnak, M.J., Rinne, J., Munger, B., Goldstein, A., Guenther, A.B., 2008. Global isoprene emissions estimated using MEGAN, ECMWF analyses and a detailed canopy environment model. *Atmos. Chem. Phys.* 8, 1329–1341.
- Nara, H., Nakagawa, F., Yoshida, N., 2006. Development of two-dimensional gas chromatography/isotope ratio mass spectrometry for the stable carbon isotopic analysis of C₂–C₅ non-methane hydrocarbons emitted from biomass burning. *Rap. Comm. Mass Spectrom.* 20, 241–247.
- Nara, H., Toyoda, S., Yoshida, N., 2007. Measurements of stable carbon isotopic composition of ethane and propane over the western North Pacific and eastern Indian Ocean: a useful indicator of atmospheric transport process. *J. Atmos. Chem.* 56, 293–314.
- Noyes, W.A., 1943. n-Butyl nitrite synthesis. In: Blatt, A.H. (Ed.), *Organic Syntheses*, vol. 2. John Wiley and Sons, Inc., New York, p. 108.
- Paulson, S.E., Flagan, R.C., Seinfeld, J.H., 1992. Atmospheric photooxidation of isoprene part I: the hydroxyl radical and ground state atomic oxygen reactions. *Int. J. Chem. Kinet.* 24, 79–101.
- Rudolph, J., Czuba, E., 2000. On the use of isotopic composition measurements of volatile organic compounds to determine the "photochemical age" of an air mass. *Geophys. Res. Lett.* 27, 3865–3868.
- Rudolph, J., Lowe, D.C., Martin, R.J., Clarkson, T.S., 1997. A novel method for compound specific determination of δ¹³C in volatile organic compounds at ppt levels in ambient air. *Geophys. Res. Lett.* 24, 659–662.
- Rudolph, J., Czuba, E., Huang, L., 2000. The stable carbon isotope fractionation for reactions of selected hydrocarbons with OH-radicals and its relevance for atmospheric chemistry. *J. Geophys. Res.* 105, 29329–29346.
- Rudolph, J., Anderson, R.S., Czapiewski, K., Czuba, E., 2003. The stable carbon isotope ratio of biogenic emissions of isoprene and the potential use of stable isotope ratio measurements to study photochemical processing of isoprene in the atmosphere. *J. Atmos. Chem.* 44, 39–55.
- Ruppert, L., Becker, K.H., 2000. A product study of the OH radical-initiated oxidation of isoprene: formation of C₅-unsaturated diols. *Atmos. Environ.* 34, 1529–1542.
- Saito, T., Tsunogai, U., Kawamura, K., Nakatsuka, T., Yoshida, N., 2002. Stable carbon isotopic compositions of light hydrocarbons over the western North Pacific and implication for their photochemical ages. *J. Geophys. Res.* 107, 4040. doi:10.1029/2000JD000127.
- Sanadze, G.A., 1969. Light-dependent excretion of molecular isoprene. *Prog. Photosynth. Res.* 2, 701–706.
- Sanadze, G.A., 2004. Biogenic isoprene (a review). *Russ. J. Plant Physiol.* 51, 729–741.
- Schnitzler, J., Graus, M., Kreuzwieser, J., Heizmann, U., Rennenberg, H., Wisthaler, A., Hansel, A., 2004. Contribution of different carbon sources to isoprene biosynthesis in poplar leaves. *Plant Physiol.* 135, 1–9.
- Schwender, J., Zeidler, J., Gröner, R., Müller, C., Focke, M., Braun, S., Lichtenthaler, F.W., Lichtenthaler, H.K., 1997. Incorporation of 1-deoxy-D-xylulose into isoprene and phytyl by higher plants and algae. *FEBS Lett.* 414, 129–134.
- Silver, C.M., Fall, R., 1991. Enzymatic synthesis of isoprene from dimethylallyl diphosphate in aspen leaf extracts. *Plant Physiol.* 97, 1588–1591.
- Sprengnether, M., Demerjian, K., Donahue, N., 2002. Product analysis of the OH oxidation of isoprene and 1,3-butadiene in the presence of NO. *J. Geophys. Res.* 107, 4268. doi:10.1029/2001JD000716.
- Stroud, C.A., Roberts, J.M., Goldan, P.D., Kuster, W.C., Murphy, P.C., Williams, E.J., Herold, D., Parrish, D., Sueper, D., Trainer, M., Fehsenfeld, F.C., Apel, E.C., Riemer, D., Wert, B., Henry, B., Fried, A., Martinez-Harder, M., Harder, H., Brune, W.H., Li, G., Xie, H., Young, V.L., 2001. Isoprene and its oxidation products, methacrolein and methyl vinyl ketone, at an urban forested site during the 1999 Southern Oxidants Study. *J. Geophys. Res.* 106, 8035–8046.
- Stroud, C.A., Roberts, J.M., Williams, E.J., Herold, D., Angevine, W.M., Fehsenfeld, F.C., Wisthaler, A., Hansel, A., Martinez-Harder, M., Harder, H., Brune, W.H., Hoenninger, G., Stutz, J., White, A.B., 2002. Nighttime isoprene trends at an urban forested site during the 1999 Southern Oxidant Study. *J. Geophys. Res.* 107. doi:10.1029/2001JD000959.
- Tingey, D.T., Manning, M., Grothaus, L.C., Burns, W.F., 1979. The influence of light and temperature on isoprene emission rates from live oak. *Physiologia Plantarum* 47, 112–118.
- Trainer, M., Williams, E.J., Parrish, D.D., Buhr, M.P., Allwine, E.J., Westburg, H.H., Fehsenfeld, F.C., Liu, S.C., 1987. Models and observations of the impact of natural hydrocarbons on rural ozone. *Nature* 329, 705–707.
- Tsunogai, U., Yoshida, N., Gamo, T., 1999. Carbon isotopic compositions of C₂–C₅ hydrocarbons and methyl chloride in urban, coastal, and maritime atmospheres over the western North Pacific. *J. Geophys. Res.* 104, 16033–16039.
- Tuazon, E.C., Atkinson, R., 1990. A product study of the gas-phase reaction of isoprene with the OH radical in the presence of NO_x. *Int. J. Chem. Kinet.* 22, 1221–1236.
- Wang, K.-Y., Shallcross, D.E., 2000. Modelling terrestrial biogenic isoprene fluxes and their potential impact on global chemical species using a coupled LSM-CTM model. *Atmos. Environ.* 34, 2909–2925.
- Warneke, C., Holzinger, R., Hansel, A., Jordan, A., Lindinger, W., Pöschl, U., Williams, J., Hoor, P., Fischer, H., Crutzen, P.J., Scheeren, H.A., Lelieveld, J., 2001. Isoprene and its oxidation products methyl vinyl ketone, methacrolein, and isoprene related peroxides measured online over the tropical rain forest of Surinam in March 1998. *J. Atmos. Chem.* 38, 167–185.
- Williams, J., Roberts, J.M., Fehsenfeld, F.C., Bertman, S.B., Buhr, M.P., Goldan, P.D., Hübler, G., Kuster, W.C., Ryerson, T.B., Trainer, M., 1997. Regional ozone from biogenic hydrocarbons deduced from airborne measurements of PAN, PPN, and MPAN. *Geophys. Res. Lett.* 24, 1099–1102.